Composites Part C: Open Access 12 (2023) 100395

Contents lists available at ScienceDirect

Composites Part C: Open Access

journal homepage: www.sciencedirect.com/journal/composites-part-c-open-access

Reversible and irreversible effects on the epoxy GFRP fiber-matrix interphase due to hydrothermal aging

Andrey E. Krauklis [a,b,*], Olesja Starkova [a], Dennis Gibhardt [c], Gerhard Kalinka [d], Hani Amir Aouissi [e,f,g], Juris Burlakovs [h], Alisa Sabalina [a], Bodo Fiedler [c]

[a] Institute for Mechanics of Materials, University of Latvia, Jelgavas street 3, Riga LV-1004, Latvia
[b] Faculty of Geography and Earth Sciences, Department of Environmental Protection, University of Latvia, Jelgavas street 1, Riga LV-1004, Latvia
[c] Hamburg University of Technology, Institute of Polymers and Composites, Denickestraße 15, Hamburg 21073, Germany
[d] Federal Institute of Materials Research and Testing (BAM), 5.3 Polymer Matrix Composites, Unter den Eichen 87, Berlin 12205, Germany
[e] Scientific and Technical Research Center on Arid Regions (CRSTRA), Biskra 07000, Algeria
[f] Laboratoire de Recherche et d'Etude en Aménagement et Urbanisme (LREAU), Université des Sciences et de la Technologie (USTHB), Algiers 16000, Algeria
[g] Environmental Research Center (CRE), Badji-Mokhtar Annaba University, Annaba 23000, Algeria
[h] Chair of Rural Building and Water Management, Estonian University of Life Sciences, Tartu 51014, Estonia

ARTICLE INFO

Keywords:
GFRP
Hydrothermal aging
Interphase
Water diffusion
Desorption
Interfacial strength

ABSTRACT

Epoxy R-Glass Fiber-Reinforced Polymer (GFRP) composite plates were hydrothermally aged at 60 °C for 23, 75, and 133 days. The water content reached 0.97 wt%, 1.45 wt% and 1.63 wt%, respectively. The studied GFRP matrix was inert to hydrolysis or chain scission, allowing for investigation of irreversible changes in the fiber-matrix interphase due to hydrothermal aging upon re-drying. During each period, a subset of the specimens was removed from the water bath and dried in a chamber. The weight loss upon drying was explained with epoxy leaching (impurities), sizing-rich interphase hydrolysis, glass fiber surface hydrolysis, accumulated degradation products escaping, and water changing state from bound to free. The influence of hydrothermal aging on the fiber-matrix interfacial properties was investigated. Lower interfacial strength of hydrothermally aged (wet) samples was attributed to plasticization of the epoxy, plasticization and degradation of the sizing-rich interphase (including formation of hydrolytic flaws), and hydrolytic degradation of the glass fiber surface. The kinetics of epoxy-compatible epoxysilane W2020 sizing-rich interphase hydrolysis provided an estimate of ca. 1.49%, 4.80%, and 8.49% of the total composite interphase degraded after 23, 75, and 133 days, respectively. At these conditions, the interface lost 39%, 48%, and 51% of its strength. Upon re-drying the specimens, a significant part of the interfacial strength was regained. Furthermore, an upward trend was observed, being 13%, 10% and 3% strength, respectively; thus, indicating a possibility of partial recovery of properties.

Introduction

Fiber Reinforced Polymers (FRPs) are widely used as structural materials in various industries, such as energy, offshore, oil and gas, marine, automotive, structural applications in civil engineering, and aerospace, due to their high strength, stiffness, light weight, and relatively good corrosion resistance compared to traditional materials, such as steel [1–6]. The superior mechanical performance of composites stems from the synergistic interaction between the three micro-constituents inside the FRP - matrix, fibers, and the interphase [1]. However, FRP structures are often exposed to environmental factors, such as water and temperature, for extended periods of time (15–40 years, or more [7]), promoting a process known as hydrothermal aging [4–9]. Hydrothermal aging is particularly critical at higher temperatures, because the aging process is accelerated [9].

Exposure of FRPs to hydrothermal environments generally results in a multiscale aging process, which has a negative impact on their mechanical performance, as the exposition of FRP to hydrothermal environments, that combine moisture and temperature, can cause chemical reactions and physical changes that affect the properties of the material, and these changes occur at multiple scales, including the molecular, microstructural, and macroscopic levels [10–12]. Consequently, the environmental durability aspect may become limiting in structural applications [13], as the superior stiffness and strength of FRPs become

* Corresponding author.
E-mail address: andykrauklis@gmail.com (A.E. Krauklis).

https://doi.org/10.1016/j.jcomc.2023.100395

Available online 29 August 2023

compromised by the uncertainty of the material-environment interaction [14,15]. Furthermore, the severity and duration of the exposure are crucial factors. For some FRPs, specifically designed and manufactured to withstand hydrothermal environments, an improved resistance to hydrothermal degradation may lead to a higher tolerance scenario, where limited exposure may occur without significant degradation [16].

Therefore, it is of utmost importance to comprehend the mechanisms and kinetics of environmental aging of individual constituents for ensuring the composite's environmental durability [9,14].

Hydrothermal aging of FRPs affects the individual micro-constituents differently (individual pathways or mechanisms) [17], which in turn leads to varying degrees of performance degradation in different FRPs [1]. Additionally, the coupled and synergistic effects between the three micro-constituents can further impact the aging rates of each component [14]. Therefore, the intricate interplay between the matrix, fibers, and interphase in FRPs requires careful consideration when investigating the effects of hydrothermal aging.

Hydrothermal aging is particularly critical for Glass Fiber-Reinforced Polymers (GFRPs) as the glass fibers (GFs) that are used in their manufacturing are hygroscopic and prone to chemical dissolution, e.g., contrary to Carbon Fiber-Reinforced Polymers (CFRPs), which are generally more inert [18,19]. Nevertheless, while GFs are generally hygroscopic, and their surface can undergo a process of dissolution, which can lead to a reduction in their diameter and strength, the extent of hygroscopicity and chemical dissolution can depend on the type of GF and the specific conditions of exposure. Furthermore, some GF types are designed to have lower levels of hygroscopicity and increased chemical resistance, making them more suitable for use in harsh environments. And this is the reason for their application, for example, in the marine and chemical industry [20].

Based on previous findings described in the authors' earlier works on hydrothermal aging of the same epoxy/glass fibers system at the same conditioning parameters (deionized (DI) water, 60 °C), several **findings** can be highlighted:

- The studied epoxy does not undergo chemical degradation, such as hydrolysis, and fully regains its mechanical properties (strength, modulus) upon redrying [21,22];
- the thermo-oxidative yellowing and leaching from the epoxy under hydrothermal conditions is known, and has no effect on the mechanical properties of the epoxy [21];
- water absorption by epoxy (and composite) follows Fickian behavior [23,24];
- hydrothermal aging results in irreversible degradation of glass fibers [25,26];
- the composite interphase undergoes irreversible property changes due to hydrolysis; their contribution increases over time; the weakening of the interphase causes the formation of hydrolytic flaws. The degradation products and water can accumulate in these flaws [17].
- the mechanical properties (ILSS, strength) of the epoxy GFRP composite decrease considerably due to the absorbed water [12,27] and these changes are only partly reversible upon water removal [28]. In this context a remaining loss of interphase strength after re-drying of about 20% was reported for a similar GF/Epoxy composite.

Based on these findings, the following **hypothesis** is put forward in this study:

Irreversible changes of the epoxy GFRP composite mechanical properties are related to the degradation of the fiber-matrix interphase (including the hydrolytic degradation of the sizing-rich interphase, and hydrolysis of glass fibers and at the surface, and subsequent void formation in the interphase [17]).

Thus, **the present study is aimed** to experimentally investigate the deterioration of the epoxy/GFRP composite interphase over time due to hydrothermal aging.

When the composite material is re-dried to its initial water content, any deterioration of mechanical properties can be attributed only to irreversibly aged micro-constituents in the material system, respectively, glass fibers, and the sizing-rich composite interphase. By using the combination of micro-constituents described above, it should be possible to investigate the hydrothermal aging of the fiber-matrix interphase. Furthermore, since the sizing-rich composite interphase contains about 70–80 wt% epoxy film former, it may be possible that some of the lost interfacial strength due to aging can be regained upon re-drying, similarly to the matrix [22].

In this study, ILSS determined via mechanical tests is selected as an indicative characteristic of the mechanical degradation of the composite interphase properties. The influence of fiber degradation is assumed to be negligible in the chosen interphase-dominant testing mode enabling the inquiry into the aging-induced mechanical property loss of the interphase. Water absorption/desorption up to 4 months after saturation was conducted at 60 °C. ILSS was determined at different time periods after water saturation and subsequent desorption cycles. Thus, the contributions of reversible and irreversible components of ILSS degradation were quantitatively estimated.

Short-beam shear (SBS) and three-point bending (3pb) are mechanical testing methods that are known to be used in evaluating the properties of a composite interphase [29]. This is because the interphase region, which is the transition zone between the fiber and matrix phases, can have a significant influence on the overall mechanical behavior of the composite material [30,31]. The fiber-matrix interphase region involves a significant influence on the shear properties of the composite material. It is well-established that the short beam shear (SBS) test method is particularly useful for evaluating the shear properties of the interphase [29]. The SBS behavior of GFRPs has been investigated by various groups, and has been shown to be an effective method of inquiry into the properties of the composite interphase [29,31,32], including the environmentally aged GFRPs [20,33]. Thus, a similar method has been chosen to mechanically characterize the composite interphase in this work.

Secondary **motivation** of this study is to further advance the reliable understanding and prediction of composite aging and property deterioration. Such progress is required in order to contribute to the reduction of testing costs and expenses leading to an increase in the validation of modeling and accelerated testing methodologies, as has been described elsewhere [15]. To achieve this, a fundamental understanding of composite aging at all levels (multiscale) is necessary [14]. While the aging of polymer matrices and fibers is more frequently explored, the degradation of the fiber-matrix interphase remains less understood. Some attempts have been made to study the kinetics of interphase aging (e.g., [17]) and the deterioration of composite properties over time [34,35], but a deeper understanding of cause and effect, as well as a mechanistic quantitative link, has yet to be established.

Materials and methods

Materials

For this study, a commonly used glass fiber epoxy GFRP material utilized in marine, oil, and gas applications was selected.

The present study utilized HiPer-Tex™ R-glass (R-GF) fabrics by 3B for reinforcement, which are produced by 3B Fibreglass located in Birkeland, Norway. The average fiber diameter of the fabrics was measured to be 17 ± 2 μm, while the density of the glass (ρ_f) was determined to be 2.54 g/cm^3, classifying the materials as high-strength and high modulus R-glass, as per international standard ISO 2078 [36]. The specific surface area of the glass fibers was 0.09 m^2/g (constituting a total surface area of 0.096 m^2 in GFRP specimens on average) [25]. According to the datasheet by 3B [37], the modulus of the R-glass utilized in this study ranged from 86 to 89 GPa.

The surface of the fibers contained the W2020 epoxysilane-rich epoxy-compatible sizing coating, which is composed of approximately

five different chemicals [38,39]. Among them is an organofunctional silane, also known as a coupling agent, which is widely regarded as the most significant component in glass fiber sizing [40–42]. This chemical class plays a critical role in enhancing adhesion and stress transfer at the fiber-matrix interphase (between the polymer matrix and the fiber) [43], while also improving the interphase strength and hydrothermal resistance of the composite [42]. According to a sizing formulation patent review by Thomason and specifically patent EP2540683A1 by Piret, Masson, and Peters of 3B, the studied W2020 sizing's coupling agent was an epoxysilane [38,39]. Typically, sizings contain approximately 10 wt% of the coupling agent [34]. The coupling agent covalently bonds the matrix to the fibers and is known to undergo irreversible hydrothermal aging, such as in the case of W2020 sizing studied here [17]. The sizing composition also includes multipurpose components such as a film former, which holds the filaments together in a strand and protects them from damage due to fiber-fiber contact. Film formers are as closely compatible with the polymer matrix as possible, and epoxies, such as those in this case, are very common film formers [40]. Typically, sizings contain around 70–80 wt% of the film former, which likely acts similarly to the matrix material of the composite [34].

The studied FRP contained a Bisphenol A diglycidyl ether (DGEBA)-based amine-cured thermoset epoxy, which is a very common matrix polymer (DGEBA epoxides constitute more than 80 to 85% of the epoxy market, according to a recent study [44]). The matrix polymer was prepared by mixing Hexion™ epoxy resin RIMR135™ and amine hardener RIMH137™ in a stoichiometric ratio of 100:30 by weight, density of matrix (ρ_m) of 1.10 g/cm^3. The resin and curing agent were composed of 63 wt% DGEBA (number average molecular weight $\leq$ 700), 14 wt% 1,6-hexanediol diglycidyl ether (HDDGE), 14 wt% poly(oxypropylene)diamine (POPA; molecular weight 230), and 9 wt% isophorondiamine (IPDA). The epoxy value of the resin ranged from 0.54 to 0.60 equivalent/100 g. The hardener had an amine value of 400–600 mg KOH/g. The mixture was degassed in a vacuum chamber for 30 min to ensure the elimination of entrapped air bubbles. As this epoxy is able to fully recover its mechanical properties upon redrying [22], it was chosen as the matrix material to enable reversible hydrothermal effects on the FRP concerning the matrix micro-constituent.

Glass fiber-reinforced epoxy composite laminates were manufactured via the vacuum-assisted resin transfer moulding (VARTM) technique, utilizing the aforementioned Hexion epoxy resin and 3B R-GF fabric. The composite laminate was subsequently sectioned into rectangular bars and cut into plates. Plate dimensions were established as 50 mm × 15 mm × 1.35 mm, with thickness tolerances maintained by means of grinding with a super-fine sandpaper (FEPA P800, grain size 21.8 μm). Specified dimensions were achieved with a precision of 5%. Laminate configuration (4 layers): +45/−45/−45/+45. The samples were cured at ambient temperature for 24 h and then subjected to post-curing in an air oven at 80 °C for 16 h. Full cure was achieved. Glass transition (T_g) of the studied epoxy is 83 ± 2 and 60 ± 2 °C in dry and saturated conditions, respectively [45]. Since the chosen wet-aging temperature was chosen around wet-T_g, physical aging should be mostly depressed and thus might be excluded from interpretation [46]. However, during the re-drying process at 60 °C, the T_g gradually increases again and the physical aging of the epoxy will take place at least during this period.

The density of the composite (ρ_{comp}) was 1.69 g/cm^3, obtained by measuring mass and dimensions of GFRP specimens. The fiber volume and mass fractions (which also includes sizing) were obtained via density measurements and calculated using Equations 1 and 2; the obtained volume and mass fractions were 0.410 and 0.616, respectively.

$$V_f = \frac{\rho_{comp} - \rho_m}{\rho_f - \rho_m} \tag{1}$$

$$m_f = \frac{\rho_f \cdot V_f}{\rho_m \cdot (1 - V_f) + \rho_f \cdot V_f} \tag{2}$$

The amount of sizing present on the fibers' surface was determined using the Loss On Ignition (LOI) method in accordance with ASTM D4963 standard [47]. However, this method may not be completely accurate and can be affected by several factors, such as the specific composition of the sizing material, the heating conditions used during the test, and the presence of any impurities or inorganic components in the fibers. It is recommended to use the method in conjunction with other analytical techniques to identify and quantify any impurities or inorganic components that may affect the LOI measurement. However, these analytical tests were not available, and thus the determined values may have an associated error. The LOI measurement was carried out at a temperature of approximately 565 °C for about 5.5 h, and the sizing was found to be 0.64 wt% of the fibers. This result is consistent with the literature, which states that the majority of industrial glass fibers have an LOI value below 1.20 wt% [43]. Zinck and Gerard also reported a similar LOI value of 0.77 wt% for a silane-based sizing they studied [48]. Therefore, the mass fraction of the interphase in the composite is LOI value times the mass fraction of the sized fibers, being ca. 0.39 wt% (of the total GFRP weight).

The composite samples were conditioned using deionized (DI) water. All of the samples were put dry into the water solutions (after drying to 0 wt%); the samples were dried at the same temperature before water immersion tests.

Methods

Water uptake tests were performed using a batch system. The epoxy GFRP plates were conditioned in a PID-controlled heated deionized water bath (60 ± 1 °C). The samples were left to condition until reaching equilibrium according to ASTM D 5229:2020, and further for the next four months. Throughout this period, samples were periodically removed from the water bath and weighed using analytical scales Mettler Toledo XS205.

The relative weight change w (%) was determined as weight gain per unit weight, Eq. (3):

$$w = 100 \times \frac{m_t - m_0}{m_0} \tag{3}$$

where m_t is the weight of the wet sample at time t, and m_0 is the weight of the reference (dry) sample. The average values are calculated using three replicates for each group of samples.

Samples were divided into 7 groups depending on their water contents and hydrothermal aging pre-history (Table 1). After a certain time (23 days, 75 days, and 133 days), a group of samples was removed from the water and stored in an oven in air for water desorption.

The following 7 configurations have been defined and experimentally tested, as indicated in Table 1.

Table 1
GFRP specimen configurations tested.

Config. ID	Configuration state
0-Initial	Dry state (properties in the initial/unaged state)
I-Wet	GFRP is saturated with water at 60°C (23 days)
I-Dried	GFRP is saturated with water at 60°C, and is re-dried
II-Wet	GFRP is subsequently aged for 2 months in the 60°C water after the saturation (75 days)
II-Dried	The GFRP has reached configuration (IV), and is subsequently re-dried and tested
III-Wet	GFRP is subsequently aged for 4 months in the 60°C water after the saturation (133 days)
III-Dried	The GFRP has reached configuration (VI), and is subsequently re-dried and tested

To investigate the influence of hydrothermal aging on the interphase aging within the composite, a mechanical testing has been performed, a method has been selected, similar to the standards ASTM D2344/D2344M [49] and DIN EN ISO 14,130 [50]. The interfacial strength S was calculated according to the Eq. (4) [49]:

$$S = 0.75 \times \frac{F}{bh} \quad (4)$$

where S is "apparent interlaminar shear strength" or "short-beam strength", MPa; F - maximum (or first jump) in force-diplacement curve, N; b,h - width and thickness in mm.

Mechanical testing of the studied epoxy GFRP specimens was performed for all 7 configurations (defined in Table 1) using Zwick Roell Z2.5 Zwick 2.5 kN (13 mm from the edge; span 22 mm; 1 mm/min).

While not being a standard SBS testing method (mixture of bending and shear failure possible), this method has been chosen because the impact of the interphase on the mechanical behavior is substantial when tested in this mode. Similar SBS tests are well known to be strongly related to interphase dominance [49,50]. To keep temperature equilibrated, the samples were tested after about 20 min after their removal from the oven.

Microscopic investigations were performed using a VHX-6500 microscope (Keyence, Japan).

Results and discussion

Water uptake and drying

Weight changes of GFRP samples during water absorption and desorption are shown in Fig. 1. Water diffusion reached a saturation after 560 h (23 days) and followed Fickian type of diffusion up to apparent saturation. The water content at apparent saturation was 0.97 wt% (Configuration I-Wet), which corresponds to matrix-related uptake of 2.52 wt%, close to what was reported for saturation before [22,46].

After the first apparent saturation, the water uptake in the GFRP continued due to the polymer chain relaxation [46], and/or increased contribution of "bound" water, and further degradation of interphase and hydrolytic flaw formation [17,51]. According to the comprehensive investigations on the water absorption behavior of the specific epoxy system [22,46,52], it is known that the maximum water absorption content cannot exceed about 3.10 wt%. Therefore, any additional water uptake in the composite must be related to the interphase region or damage in terms of voids, flaws and debondings, which give space for water absorption. As fiber/matrix debonding occurs due to hydrothermal aging, flaws and cracks are opening, which can be filled with additional water over time [46]. Analyzing the absorption and desorption curves in Fig. 1, it becomes clear that the water uptake from stage II onwards has to be based on additional damage in the composite (more details in chapter 3.3). After additional aging of about two (Configuration II-wet) and four months (Configuration III-wet), 1807 h (75 days) and 3197 h (133 days), respectively, the water content reaches 1.45 wt %, and 1.63 wt% (3.78 wt% and 4.24 wt% of matrix fraction), respectively.

At the first stage of sorption, water enters the samples mainly by diffusion, filling the free volume of the epoxy resin. Therefore, the sorption curve in section 0-I is described by Fick's law. The samples also undergo irreversible changes due to hydrothermal aging, the contribution of which increases with increasing exposure time of the samples in hot water. Such changes can occur at the fiber-matrix interphase (including sizing-rich interphase and the glass fiber surface). The formation of voids and debondings in the interface contributes to the inflow of additional water, which can form into clusters. The experimental evidence of the "formation of voids" or "debonding in the interface" of the same material system is described in a previous study [17]. However, the study did not address the deterioration of the mechanical properties, and proposed it as the future work. Therefore, this study is a direct continuation. Therefore, in section II-III, a continuous increase in the mass of the samples is observed, similarly to [17,53].

Drying has been performed resulting in configurations I-Dried, II-Dried and III-Dried. For those, the weight change was determined to be 0.14 wt%, −0.05 wt%, and −0.29 wt%, respectively. The difference after re-drying is interpreted to be due to (a) epoxy leaching, (b) sizing-rich interphase hydrolysis, and (c) glass fiber surface hydrolysis.

As was mentioned earlier, the epoxy does not undergo hydrolysis, and its strength can be fully regained upon redrying [22]. However, epoxy leaching may affect the weight loss slightly, even though it has no significant effect on mechanical properties [21]. Leaching follows Fickian diffusion. According to [21], epoxy leaching of the studied epoxy involves unreacted epicholorohydrin and ionic impurities with a total leachable amount being estimated at 0.092 wt% of the matrix [17]. Therefore, leaching from epoxy could explain only up to a maximum weight loss of 0.035 wt% of the GFRP.

The hydrolysis kinetics of the W2020 sizing-rich interphase reported in [17] provide an estimate of 1.80×10^{-7} g/h (kinetic constant 1.98 ×

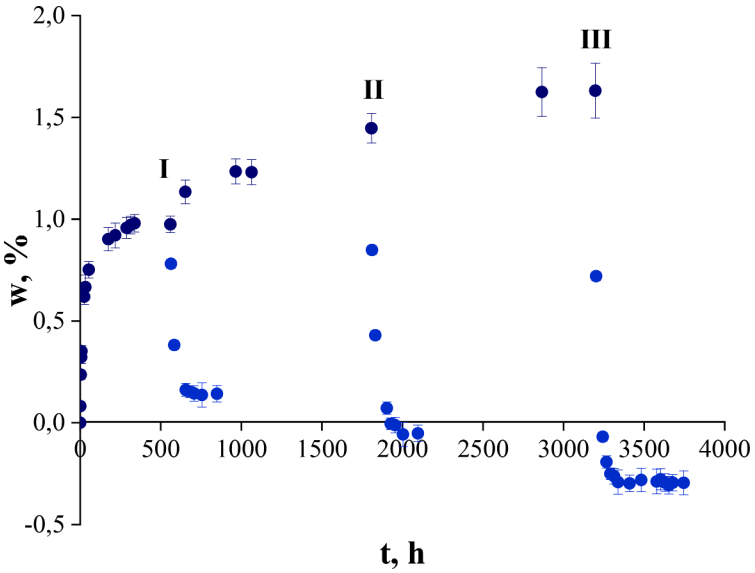

Fig. 1. Weight changes of GFRP samples during water absorption and desorption (dark blue: sorption, bright blue: desorption).

10^{-7} g/m^{2}h) loss under similar hydrothermal aging conditions. Therefore, it can be estimated that the loss of the composite interphase at configuration I (560 h), II (1807 h) and III (3197 h) were ca. 1.01 × 10^{-4}, 3.25 × 10^{-4}, and 5.75 × 10^{-4} g, respectively. The mass fraction of the interphase in the composite was ca. 0.39 wt% of the total GFRP weight (see Materials section), and the average mass of a GFRP specimen was 1.7363 g. Thus, on average, a GFRP plate contained 0.68 × 10^{-2} g interphase. The hydrothermal aging-induced mass loss of the interphase on average is estimated only to 1.49%, 4.80%, and 8.49% of the sizing-rich W2020 interphase degraded at configurations I, II, and III, respectively. Therefore, at Stage III, the hydrolysis of sizing could explain up to 0.033 wt% loss of GFRP weight.

Furthermore, based on the kinetics of R-GF fiber dissolution from the epoxy GFRP under hydrothermal conditions (DI, 60 °C) [54], the hydrolytic glass material loss is estimated at the maximum up to 0.044 wt% of GFRP weight (after 3197 h; kinetic constant of glass hydrolysis 5.35 • 10^{-10} g/(m^2•s) under similar conditions [54]). However, it is important to note, that the kinetics of glass dissolution can capture only the ions leaching from glass that can escape the GFRP into the surrounding water (due to specifics of the ICP-MS method [54]); Therefore, the kinetics described are apparent (lower than true kinetics), since a significant number of ions accumulate inside the GFRP and cannot be measured. The largest contribution to weight loss was mainly due to fiber degradation as has been shown by Gibhardt et al. in a recent study, where it was observed how the fibers degrade as the cracks are opening [12].

Based on these estimates of (a) epoxy leaching (ca. −0.035 wt%), (b) sizing-rich interphase hydrolysis (ca. −0.033 wt%), and (c) glass fiber surface hydrolysis (ca. −0.044 wt%), a total explained weight loss (by these three factors) constitutes ca. −0.112 wt%. However, experimentally a weight loss of −0.29 wt% has been observed (Fig. 1). Therefore, the difference of 0.178 wt% remains unexplained. Some of the possible explanations are hypothesized, and should be explored in the future in more detail.

In areas with extensive defects and cracks, and hence with a large amount of water. The water hydrolytically attacks the interphase between fibers and matrix, as well as the fiber surface itself [17]. Due to the hydrolysis of the interface and the fibers, some components may be leached out. However, the degradation products (of both fibers and interphase) cannot easily move along the interphase and escape into the surrounding water at the composite's surface [17]. Instead, the weakening of the interphase causes the formation of flaws. The degradation products and water can accumulate in these flaws along with the water [17]. The effect of drying has not been investigated in the previous study [17]. It is possible, that along with the desorption of water in the drying cycle, some of the degradation products can escape resulting in the further weight loss. It is, thus, speculated that this effect is contributing to the remaining unexplained weight loss of −0.178 wt%. Additional contribution to the remaining unexplained loss could be due to the effect of bound water, as described further.

Let us assume that the increase in mass is associated with an additional flow of water into regions with voids, their association into clusters and bounding. To model this behavior, the Langmuir model is used.

The Langmuir two-phase model considers a free diffusion phase and a bound phase of a penetrant that does not involve diffusion. The Langmuir model is given by Eq. (5) [55,56]:

$$w(t) = w_\infty \left[1 - \frac{\beta}{\beta+\gamma} G(t) - \frac{\gamma}{\beta+\gamma} \exp(-\beta t)\right] \quad (5)$$

where γ is the probability per unit time that a mobile molecule will become bound, and β is the probability per unit time that a bound molecule will become mobile. w_∞ is the saturation water content.

G(t) is given by Eq. (6):

$$G(t) = \exp\left[-7.3\left(\frac{Dt}{h^2}\right)^{0.75}\right] \quad (6)$$

where D is the diffusion coefficient, and h is thickness of the sample.

According to Eq. (5)-(6), when β = 1 and γ = 0, the two-phase model reduces to the single-phase case, i.e., Fickian diffusion model.

Fig. 2 shows the experimental water absorption curve (weight change with the square root of time) and its description using the Fick and Langmuir models Eqs. (5,6). The model parameters take the following values: D = 0.0055 mm^2/h, w_∞(Fick) = 0.96%, w_∞(Langmuir) = 3.36%, β = 1•10^{-4} h^{-1}, γ = 2.5•10^{-4} h^{-1}. As can be observed from Fig. 2, the Fick model is only suitable for the initial 0-I water absorption period, while the Langmuir model gives a reasonable approximation to the subsequent I-II stage.

Water desorption for the studied epoxy GFRP follows Fick's law [23]. That is, when the samples are dried, only free water comes out. Therefore, a residual mass of samples (irreversibility of sorption-desorption) is often observed, which is associated with the amount of bound water in the sample [57]. The leaching out of any components during sorption, on the contrary, leads to excessive weight loss (negative mass change) of the samples during their drying [21]. It can be seen from Fig. 1 that not all water is desorbed during the first drying of the samples and the residual w of I-Dry samples is 0.14%. Note that the sorption in this region proceeded according to the Fick diffusion law without a noticeable contribution of bound water (Fig. 2). It can be assumed that this non-desorbed water is bound water (according to the Langmuir formulation), initially present in the samples and/or formed during the sorption process. In the second stage of desorption (II), the weight of the samples practically returns to the initial value, and in the third stage (III), there is excessive weight loss. Since, as noted above, the leaching of degradation products cannot fully explain such weight loss, this behavior can be explained by the release of additional water from the samples. The hydrolytic degradation processes of sizing-rich interphase and glass fiber surface, and the accompanying reorganization of the accumulation and state of absorbed water led, on the one hand, to additional absorption (more clustered water), and, on the other hand, contributed to the transition of bound water into free water (according to Langmuir's concept). That water, which was initially considered to be bound and for the removal of which additional energy (temperature) was needed, has now become available for desorption.

Fig. 3 shows desorption data (actual weight loss of the samples). As can be seen, the data are well described by Fick's law. Note that the

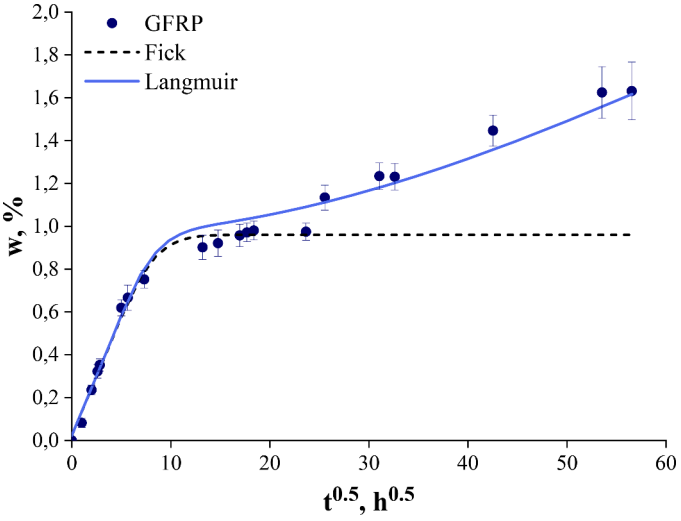

Fig. 2. Weight changes of GFRP samples and their approximation by Fick's and Langmuir models.

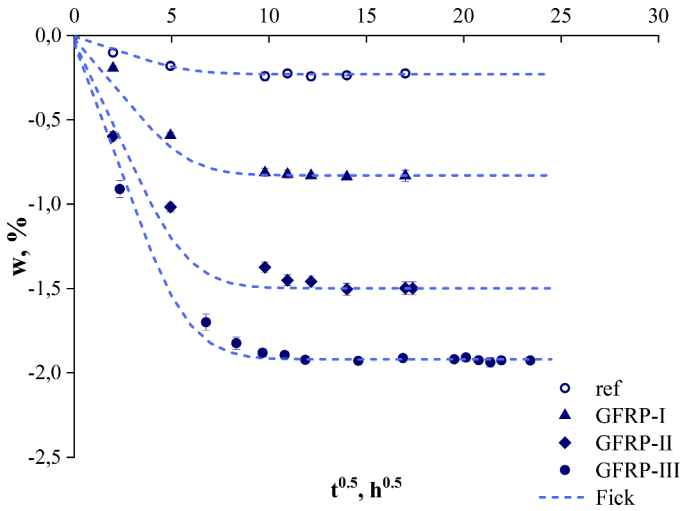

Fig. 3. Weight changes of GFRP samples during desorption started at different times after saturation.

desorption rate is the same in all cases and the diffusion coefficient $D = 0.011$ mm^2/h. This indicates the same mechanism for the release of water (free water) from the samples. Note that the rate of desorption is 2 times higher than the rate of sorption. Similar results have been reported in other papers [55,58].

Loss of interfacial strength

The obtained interfacial strength results are summarized in Fig. 4 and Table 2 showing the average and standard deviations of 3 parallels for each GFRP configuration.

The load-displacement curves are provided for all 7 defined configurations in Fig. 5 (the curve closest to the average out of 3 parallels chosen as representative for each configuration). where w (%) stands for water content, and S (MPa) for interfacial strength.

Table 2 reports the interfacial strength in initial dry configuration, as well as in configurations I, II, and III in both wet and dried states, indicating the reversible and irreversible components.

The trend of interfacial strength deterioration in the wet state shows a continuous interfacial strength loss with time, and is in harmony with findings by Rocha et al. [28]. They have found that the decrease in strength is rapid in the beginning, and slows down with time

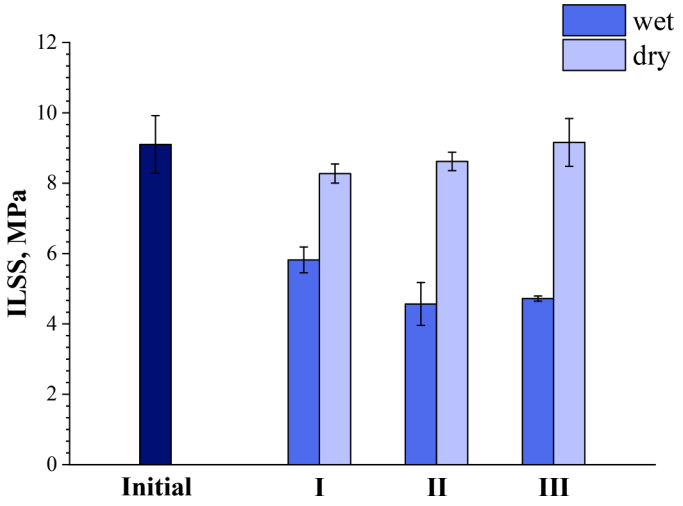

Fig. 4. Interfacial strength of the studied epoxy GFRPs at 7 defined configurations.

Table 2
Water contents and interfacial strength measured for all 7 configurations. .

Configuration	w, %	S, MPa	S loss, %	S loss components
0	0	9.54 ± 0.43	-	-
I - Wet	0.97 ± 0.04	5.82 ± 0.37	39	Reversible: 2.45 MPa (26% regained) Irreversible: 1.27 MPa (13% lost)
I - Dried	0.14 ± 0.03	8.27 ± 0.27	13	
II - Wet	1.45 ± 0.07	4.93 ± 0.37	48	Reversible: 3.69 MPa (39% regained) Irreversible: 0.92 MPa (10% lost)
II - Dried	−0.05 ± 0.01	8.62 ± 0.26	10	
III - Wet	1.63 ± 0.13	4.72 ± 0.07	51	Reversible: 4.57 MPa (48% regained) Irreversible: 0.25 MPa (3% lost)
III - Dried	−0.29 ± 0.04	9.29 ± 0.48	3	

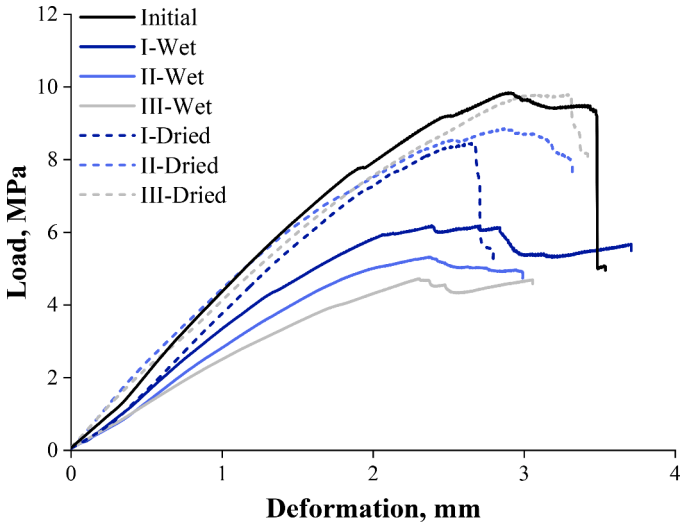

Fig. 5. Interfacial strength ILSS-deformation curves for 3 parallels for each of the 7 configurations.

(degradation is slowed down with time) [28].

The hydrothermal aging-induced mass loss of the sizing-rich interphase was estimated using the chemical kinetics of W2020 hydrolysis [17], and were ca. 1.49%, 4.80%, and 8.49% of the total composite interphase degraded at configurations I (560 h), II (1807 h) and III (3197 h), respectively. The interface lost 39%, 48%, and 51% of its strength loss at these conditions, according to the experimental results. Lower ILSS of hydrothermally aged (wet) samples can be attributed to several factors: (a) plasticization of the epoxy matrix; (b) plasticization and degradation of the sizing-rich interphase, including formation of hydrolytic flaws and deterioration of strength transfer between the fiber and the matrix; (c) hydrolytic degradation of the glass fiber surface.

Upon re-drying the specimens, a significant part of the interfacial strength was regained. Furthermore, an upward trend was observed, being 13%, 10% and 3% strength loss at I-Dried, II-Dried, and III-Dried, respectively.

The Interfacial strength vs. water content is plotted in Fig. 6.

Upon re-drying, the mechanical properties of the epoxy matrix are fully regained (plasticization effect is recovered after redrying of samples), according to [22]. Therefore, the effect of fiber-matrix interphase degradation (hydrolysis of sizing-rich phase and fiber surface) remains [17,26]. Assuming, as was previously described, that the tests were performed in the interface-dominant mode, the loss of interfacial

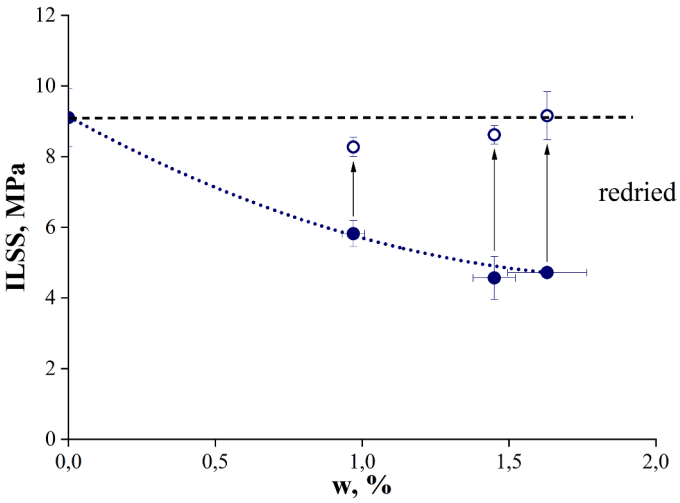

Fig. 6. Interfacial strength vs. water content. Unfilled symbols refer to re-dried samples.

strength is showcased by configurations I-Dried, II-Dried, and III-Dried states, indicating a decrease of 13%, 10%, and 3%, respectively. The decreased ILSS of dried samples (conditionally assumed as "dry") can be related to: (a) the irreversible hydrolytic degradation of the fiber-matrix interphase, and (b) remained bound water (if some bound water remains, we can still observe plasticizing effects). The upwards trend is unexpected, and is speculated to be possibly related to partial self-healing of the composite interphase (partial rebinding of the silanes and hydrogen to the glass fiber surface) [59,60]. This is considered possible, since only ca. 8.49% of the sizing-rich composite interphase degraded at stage III, as estimated. However, further research is required to confirm this hypothesis.

It should be noted, that the measured interfacial strength was very low (<10 MPa), which was likely due to the imperfect selection of the testing method for the desired sample geometry. Nevertheless, the differences in the strength related to the state and conditioning duration were well observed and exhibited a clear trend. It was not clear if the specimens have failed in pure shear mode via visual inspection alone. However, a further analysis of the damage of the samples was done by microscopy to shed some light on this problem.

Optical microscopy

The microscopy has shown that the delamination failure was dominant. The failure measured was not tensile, nor compressive (not bending mode). Thus, the failure was the result of the shear mode, and the interpretation was such, that indeed the interfacially-dominant property was measured. The observation was valid for specimens tested in both dry and wet configurations, as shown in Fig. 7. Only slight crushing occurred in the case of a dry specimen. Furthermore, the delamination originated from the half-way of the support, thus confirming that the delamination failure occurred under the shear mode (interfacially-dominant).

Further work on establishing the quantitative link between the chemical kinetics of the hydrothermal aging of the interphase and its effect on interfacial strength loss is required, and should also consider other methods of inquiry of interfacial strength testing, e.g., by single fiber pull-out tests, similarly to [61] or using the direct interphase analysis methods (i.e. local measurements described in [62]).

Conclusions

The influence of hydrothermal aging on fiber-matrix interfacial properties (ILSS) of a R-glass epoxy GFRP was investigated.

Sorption followed Fick's law. The apparent saturation was reached after 23 days at 60 °C. The water content reached 0.97 wt%. After 75 days and 133 days, the water content reached 1.45 wt% and 1.63 wt%, respectively. The absorption process did not have any effect on rates of desorption (desorption proceeded with equal rates at all stages).

Drying has been performed resulting in weight change of 0.14 wt%, −0.05 wt%, and −0.29 wt%, respectively. The weight loss was due to (a) epoxy leaching, (b) sizing-rich interphase hydrolysis, and (c) glass fiber surface hydrolysis. However, these processes could explain weight loss only up to −0.112 wt%. The remaining difference of 0.178 wt% was attributed to the following possible mechanisms: (a) some accumulated degradation products (sizing; glass) inside the GFRP could escape along with the desorbed water in the drying cycle; (b) water changing state from bound to free. However, both hypotheses require additional investigation.

The changes of the mechanical properties (ILSS) were related to the degradation of the fiber-matrix interphase. Lower ILSS of hydrothermally aged (wet) samples was attributed to: (a) plasticization of the epoxy matrix; (b) plasticization and degradation of the sizing-rich interphase, including formation of hydrolytic flaws and deterioration of strength transfer between the fiber and the matrix; and (c) hydrolytic degradation of the glass fiber surface. The kinetics of W2020 hydrolysis provided an estimate of ca. 1.49%, 4.80%, and 8.49% of the total composite interphase degraded after 23, 75, and 133 days, respectively. At these conditions, the interface lost 39%, 48%, and 51% of its strength. Upon re-drying the specimens, a significant part of the interfacial strength was regained. The decreased ILSS of dried samples was related to: (a) the irreversible hydrolytic degradation of the fiber-matrix interphase, and (b) remained bound water (if some bound water remains, we can still observe plasticizing effects). Furthermore, an upward trend was observed, being 13%, 10% and 3% strength, respectively. Thus, indicating a possibility of partial self-healing of the composite interphase (partial rebinding of the silanes to the glass fiber surface), although

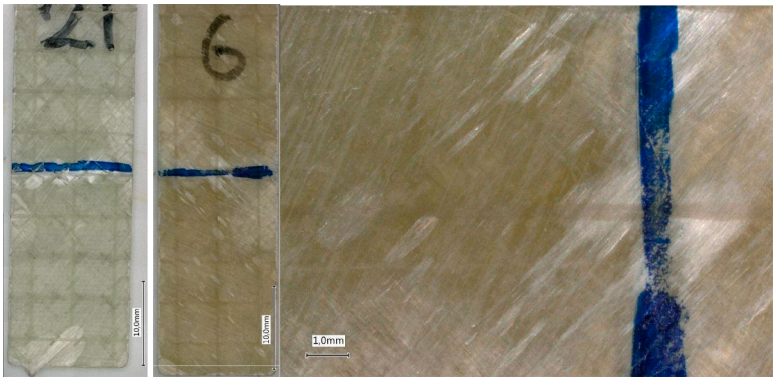

Fig. 7. Microscopy of GFRP specimens showing signs of delamination (left: dry configuration; right: wet aged configuration).

additional evidence is required to confirm such hypothesis.

Funding

This research was funded by the European Regional Development Fund within the Activity 1.1.1.2 “Post-doctoral Research Aid” of the Specific Aid Objective 1.1.1 of the Operational Programme “Growth and Employment” (Nr.1.1.1.2/VIAA/4/20/606, “Modelling Toolbox for Predicting Long-Term Performance of Structural Polymer Composites under Synergistic Environmental Ageing Conditions”).

CRediT authorship contribution statement

Andrey E. Krauklis: Conceptualization, Methodology, Formal analysis, Investigation, Resources, Data curation, Writing – original draft, Writing – review & editing, Validation, Visualization, Supervision, Project administration, Funding acquisition. **Olesja Starkova:** Conceptualization, Methodology, Formal analysis, Data curation, Writing – review & editing, Validation, Visualization, Supervision. **Dennis Gibhardt:** Formal analysis, Resources, Writing – review & editing, Validation, Visualization. **Gerhard Kalinka:** Formal analysis, Resources, Writing – review & editing, Validation, Supervision. **Hani Amir Aouissi:** Writing – review & editing, Validation. **Juris Burlakovs:** Writing – review & editing, Validation. **Alisa Sabalina:** Formal analysis, Writing – review & editing, Validation, Supervision. **Bodo Fiedler:** Resources, Writing – review & editing, Validation, Supervision.

Declaration of Competing Interest

The authors declare that they have no known competing financial interests or personal relationships that could have appeared to influence the work reported in this paper.

Data availability

Data will be made available on request.

Acknowledgments

This work was supported by the European Regional Development Fund within the Activity 1.1.1.2 “Post-doctoral Research Aid” of the Specific Aid Objective 1.1.1 of the Operational Programme “Growth and Employment” (Nr.1.1.1.2/VIAA/4/20/606, “Modelling Toolbox for Predicting Long-Term Performance of Structural Polymer Composites under Synergistic Environmental Ageing Conditions”). Andrey is grateful to Luc Peters of 3B for kindly providing the fiberglass. Andrey is especially grateful to Oksana.

References

[1] J. Berg, F.R. Jones, The role of sizing resins, coupling agents and their blends on the formation of the interphase in glass fiber composites, Compos. Part A-Appl. S 29 (1998) 1261–1272, https://doi.org/10.1016/S1359-835X(98)00091-8.
[2] G.Z. Xiao, M.E.R. Shanahan, Swelling of DGEBA/DDA epoxy resin during hygrothermal ageing, Polymer (Guildf) 39 (1998) 3253–3260, https://doi.org/10.1016/S0032-3861(97)10060-X.
[3] A. Toscano, G. Pitarresi, M. Scafidi, M. Di Filippo, G. Spadaro, S. Alessi, Water diffusion and swelling stresses in highly crosslinked epoxy matrices, Polym. Degrad. Stab. 133 (2016) 255–263, https://doi.org/10.1016/j.polymdegradstab.2016.09.004.
[4] I. Grabovac, D. Whittaker, Application of bonded composites in the repair of ships structures—A 15-year service experience, Compos. Part A-Appl. S 40 (2009) 1381–1398, https://doi.org/10.1016/j.compositesa.2008.11.006.
[5] C.G. Gustafson, A. Echtermeyer, Long-term properties of carbon fibre composite tethers, Int. J. Fatigue 28 (2006) 1353–1362, https://doi.org/10.1016/j.ijfatigue.2006.02.035.
[6] Advanced Fiber-reinforced Polymer (FRP) Composites for Structural Applications, J. Bai Ed., Woodhead Publishing Series in Civil and Structural Engineering.
[7] D. McGeorge, A.T. Echtermeyer, K.H. Leong, B. Melve, M. Robinson, K.P. Fischer, Repair of floating offshore units using bonded fibre composite materials, Compos. Part A-Appl. S 40 (2009) 1364–1380, https://doi.org/10.1016/j.compositesa.2009.01.015.
[8] I.B.C.M. Rocha, F.P. van der Meer, S. Raijmaekers, F. Lahuerta, R.P.L. Nijssen, L. P. Mikkelsen, L.J. Sluys, A combined experimental/numerical investigation on hygrothermal aging of fiber-reinforced composites, Eur. J. Mech. A-Solids 73 (2019) 407–419, https://doi.org/10.1016/j.euromechsol.2018.10.003.
[9] A. Echtermeyer, A. Gagani, A. Krauklis, M. Tobiasz, Multiscale modelling of environmental degradation—first steps, in: P. Davies, Y. Rajapakse (Eds.), Durability of Composites in a Marine Environment 2. Solid Mechanics and Its Applications, Springer, Cham, 2018, pp. 135–149, https://doi.org/10.1007/978-3-319-65145-3_8, 245.
[10] Y.J. Weitsman, M. Elahi, Effects of fluids on the deformation, strength and durability of polymeric composites—An overview, Mech. Time-Depend Mater. 4 (2000) 107–126, https://doi.org/10.1023/A:1009838128526.
[11] S. Roy, Moisture-induced degradation, in: V.K. Pochiraju, P.G. Tandon, A. G. Schoppner (Eds.), Long-Term Durability of Polymeric Matrix Composites, Springer, Boston, MA, USA, 2012, pp. 181–236. ISBN:978-1-4419-9307-6.
[12] D. Gibhardt, A. Doblies, L. Meyer, B. Fiedler, Effects of hygrothermal ageing on the interphase, fatigue, and mechanical properties of glass fibre reinforced epoxy, Fibers 7 (2019) 55, https://doi.org/10.3390/fib7060055.
[13] M. Wang, X. Xu, J. Ji, Y. Yang, J. Shen, M. Ye, The hygrothermal aging process and mechanism of the novolac epoxy resin, Compos. Part B-Eng. 107 (2016) 1–8, https://doi.org/10.1016/j.compositesb.2016.09.067.
[14] A.E. Krauklis, C.W. Karl, I.B.C.M. Rocha, J. Burlakovs, R. Ozola-Davidane, A. I. Gagani, O. Starkova, Modelling of environmental ageing of polymers and polymer composites—Modular and multiscale methods, Polymers (Basel) 14 (2022) 216, https://doi.org/10.3390/polym14010216.
[15] O. Starkova, A.I. Gagani, C.W. Karl, I.B.C.M. Rocha, J. Burlakovs, A.E. Krauklis, Modelling of environmental ageing of polymers and polymer composites—Durability prediction methods, Polymers (Basel) 14 (2022) 907, https://doi.org/10.3390/polym14050907.
[16] K. Mayandi, N. Rajini, Nadir Ayrilmis, M.P. Indira Devi, Suchart Siengchin, Faruq Mohammad, Hamad A. Al-Lohedan, An overview of endurance and ageing performance under various environmental conditions of hybrid polymer composites, J. Mater. Res. Technol. 9 (6) (2020) 15962–15988, https://doi.org/10.1016/j.jmrt.2020.11.031.
[17] A. Krauklis, A. Gagani, A. Echtermeyer, Long-term hydrolytic degradation of the sizing-rich composite interphase, Coatings 9 (2019) 263, https://doi.org/10.3390/coatings9040263.
[18] A.T. DiBenedetto, Tailoring of interfaces in glass fiber reinforced polymer composites: a review, Mater. Sci. Eng. A 302 (2001) 74–82, https://doi.org/10.1016/S0921-5093(00)01357-5.
[19] A.T. Echtermeyer, A.E. Krauklis, A.I. Gagani, E. Sæter, Zero stress aging of glass and carbon fibers in water and oil—strength reduction explained by dissolution kinetics, Fibers 7 (2019) 107, https://doi.org/10.3390/fib7120107.
[20] J. Thomason, G. Xypolias, Hydrothermal ageing of glass fibre reinforced vinyl ester composites: a review, Polymers (Basel) 15 (2023) 835, https://doi.org/10.3390/polym15040835.
[21] A. Krauklis, A. Echtermeyer, Mechanism of yellowing: carbonyl formation during hygrothermal aging in a common amine epoxy, Polymers (Basel) 10 (2018) 1017–1031, https://doi.org/10.3390/polym10091017.
[22] A.E. Krauklis, A.I. Gagani, A.T. Echtermeyer, Hygrothermal aging of amine epoxy: reversible static and fatigue properties, Open Eng. 8 (2018) 447–454, https://doi.org/10.1515/eng-2018-0050.
[23] A.E. Krauklis, A.I. Gagani, A.T. Echtermeyer, Near-infrared spectroscopic method for monitoring water content in epoxy resins and fiber-reinforced composites, Materials (Basel) 11 (2018) 586, https://doi.org/10.3390/ma11040586.
[24] A.I. Gagani, Y. Fan, A.H. Muliana, A.T. Echtermeyer, Micromechanical modeling of anisotropic water diffusion in glass fiber epoxy reinforced composites, J. Compos. Mater. 52 (2017) 2321–2335.
[25] A.E. Krauklis, A.T. Echtermeyer, Long-term dissolution of glass fibers in water described by dissolving cylinder zero-order kinetic model: mass loss and radius reduction, Open Chem. 16 (2018) 1189–1199, https://doi.org/10.1515/chem-2018-0133.
[26] A.E. Krauklis, A.I. Gagani, K. Vegere, I. Kalnina, M. Klavins, A.T. Echtermeyer, Dissolution kinetics of R-glass fibres: influence of water acidity, temperature, and stress corrosion, Fibers 7 (2019) 22, https://doi.org/10.3390/fib7030022.
[27] A.I. Gagani, A.E. Krauklis, E. Sæter, N.P. Vedvik, A.T. Echtermeyer, A novel method for testing and determining ILSS for marine and offshore composites, Compos. Struct. 220 (2019) 431–440, https://doi.org/10.1016/j.compstruct.2019.04.040.
[28] I.B.C.M. Rocha, S. Raijmaekers, R.P.L. Nijssen, F.P. van der Meer, L.J. Sluys, Hygrothermal ageing behaviour of a glass/epoxy composite used in wind turbine blades, Compos. Struct. 174 (2017) 110–122, https://doi.org/10.1016/j.compstruct.2017.04.028.
[29] M. Jurko, L. Souckova, J. Prokes, V. Cech, The effect of glass fiber storage time on the mechanical response of polymer composite, Polymers (Basel) 14 (2022) 4633, https://doi.org/10.3390/polym14214633.
[30] L. Yang, J.L. Thomason, Effect of silane coupling agent on mechanical performance of glass fibre, J. Mater. Sci. 48 (2013) 1947–1954, https://doi.org/10.1007/s10853-012-6960-7.
[31] P. Kumar, R. Chandra, S.P. Singh, Interphase effect on fiber-reinforced polymer composites, Compos. Interface 17 (2010) 15–35, https://doi.org/10.1163/092764409X12580201111502.

[32] Gowthaman Swaminathan, Chandrakumar Palanisamy, Gowrisankar Chidambaram, Gaëlle Henri, Chandrasekhar Udayagiri, Enhancing the interfacial strength of glass/epoxy composites using ZnO nanowires, Compos. Interface 25 (2018), https://doi.org/10.1080/09276440.2017.1341790.
[33] W.T. Barker. Short beam shear strength evaluations of GFRP composites: correlations through accelerated and natural aging. Graduate Theses, Dissertations, and Problem Reports. 2019, 3776. https://researchrepository.wvu.edu/etd/3776.
[34] Y. Joliff, L. Belec, J.F. Chailan, Impact of the interphases on the durability of a composite in humid environment – a short review, in: Proc. 20th Int. Conf. Composite Structures ICCS20, Paris, France, 2017.
[35] L. Riaño, L. Belec, J.F. Chailan, Y. Joliff, Effect of interphase region on the elastic behavior of unidirectional glass-fiber/epoxy composites, Compos. Struct. 198 (2018) 109–116, https://doi.org/10.1016/j.compstruct.2018.05.039.
[36] International Standard ISO 2078:1993 (revised in 2014), Textile glass – Yarns – Designation, 2014.
[37] 3B Fibreglass data sheet. https://www.3b-fibreglass.com/HiPer-tex (last accessed on 6 April 2023).
[38] W. Piret, N. Mason, L. Peters. European Patent EP2540683A1. Glass fibre sizing composition by 3B-Fibreglass SPRL, 2011.
[39] J.L. Thomason, Glass Fibre Sizing: A Review of Size Formulation Patents, Blurb Co, Glasgow, Scotland, UK, 2015. ISBN:978-0-9573814-3-8.
[40] K.L. Loewenstein, Glass science and technology (Book 6). The Manufacturing Technology of Continuous Glass Fibres, Elsevier, Amsterdam, Netherlands, 1993. ISBN:978-0444893468.
[41] J.L. Thomason, L.J. Adzima, Sizing up the interphase: an insider's guide to the science of sizing, Compos. Part A-Appl. S 32 (2001) 313–321, https://doi.org/10.1016/S1359-835X(00)00124-X.
[42] E.P. Plueddemann, Silane Coupling Agents, 2nd edition, Plenum Press, New York and London, 1991. ISBN:978-0-306-43473-0.
[43] J.L. Thomason, Glass Fiber Sizings: A Review of the Scientific Literature. Middletown, DE, USA, 2012. ISBN:978-0-9573814-1-4.
[44] N. Karak, Sustainable Epoxy Thermosets and Nanocomposites, 1385, American Chemical Society, Washington, DC, 2021, https://doi.org/10.1021/bk2021-1385.
[45] A.E. Krauklis, A.G. Akulichev, A.I. Gagani, A.T. Echtermeyer, Time–temperature–plasticization superposition principle: predicting creep of a plasticized epoxy, Polymers (Basel) 11 (2019) 1848, https://doi.org/10.3390/polym11111848.
[46] D. Gibhardt, C. Buggisch, D. Meyer, B. Fiedler, Hygrothermal aging history of amine-epoxy resins: effects on thermo-mechanical properties, Front. Mater. 9 (2022), 826076, https://doi.org/10.3389/fmats.2022.826076.
[47] ASTM D4963/D4963M-2011. Standard Test Method For Ignition Loss of Glass Strands and Fabrics, 2011.
[48] P. Zinck, J.F. Gerard, On the hybrid character of glass fibres surface networks, J. Mater. Sci. 40 (2005) 2759–2760, https://doi.org/10.1007/s10853-005-2124-3.
[49] ASTM d-2344ASTM D2344 - Standard Test Method for Short-Beam Strength of Polymer Matrix Composite Materials and Their Laminates.
[50] DIN EN ISO 14130. Fibre-reinforced plastic composites — Determination of apparent interlaminar shear strength by short-beam method, 2018.
[51] D. Gibhardt, C. Fleschhut, B. Fiedler, The influence of different glass fiber/epoxy matrix combinations on the durability under severe moisture impact, IOP Conf. Ser.: Mater. Sci. Eng. 942 (2020), 012009, https://doi.org/10.1088/1757-899X/942/1/012009.
[52] D. Gibhardt, A.E. Krauklis, A. Doblies, A. Gagani, A. Sabalina, O. Starkova, B. Fiedler, Time, temperature and water aging failure envelope of thermoset polymers, Polym. Test 118 (2023), 107901, https://doi.org/10.1016/j.polymertesting.2022.107901.
[53] D. Perreux, D. Choqueuse, P. Davies, Anomalies in moisture absorption of glass fibre reinforced epoxy tubes, Compos. Part A-Appl. S 33 (2002) 147–154, https://doi.org/10.1016/S1359-835X(01)00111-7.
[54] A.E. Krauklis, H.A. Aouissi, S. Bencedira, J. Burlakovs, I. Zekker, I. Bute, M. Klavins, Influence of environmental parameters and fiber orientation on dissolution kinetics of glass fibers in polymer composites, J. Compos. Sci. 6 (2022) 210, https://doi.org/10.3390/jcs6070210.
[55] C. Gao, C. Zhou, Moisture absorption and cyclic absorption–desorption characters of fibre-reinforced epoxy composites, J. Mater. Sci. 54 (2019) 8289–8301, https://doi.org/10.1007/s10853-019-03399-7.
[56] O. Starkova, M.A. Aiello, A. Aniskevich, Long-term moisture diffusion in vinylester resin and CFRP rebars: a 20-year case study, Compos. Sci. Technol. (2023), 110167, https://doi.org/10.1016/j.compscitech.2023.110167.
[57] J. Zhou, J.P. Lucas, Hygrothermal effects of epoxy resin. Part I: the nature of water in epoxy, Polymer (Guildf) 40 (1999) 5505–5512, https://doi.org/10.1016/S0032-3861(98)00790-3.
[58] Y.C. Lin, Xu Chen, Moisture sorption–desorption–resorption characteristics and its effect on the mechanical behavior of the epoxy system, Polymer (Guildf) 46 (2005) 11994–12003, https://doi.org/10.1016/j.polymer.2005.10.002.
[59] J. Xie, K. Chen, M. Yan, J. Guo, Q. Xie, F. Lü, Effect of temperature and water penetration on the interfacial bond between epoxy resin and glass fiber: a molecular dynamics study, J. Mol. Liq. 350 (2022), 118424, https://doi.org/10.1016/j.molliq.2021.118424.
[60] Private communication with 3B Fibreglass, 2023.
[61] É.S.S. Guerra, B.L. Silva, J.D.D. Melo, G. Kalinka, A.P.C. Barbosa, Microscale evaluation of epoxy matrix composites containing thermoplastic healing agent, Compos. Sci. Technol. 232 (2023), https://doi.org/10.1016/j.compscitech.2022.109843.
[62] M. Saber, H. Hosseini-Toudeshky, Interphase elastic modulus characterization in glass/epoxy composite using combined peridynamics and experimental method, J. Reinf. Plast. Comp. (2023), https://doi.org/10.1177/07316844231155091.